TU Delft

Delft University of Technology

Document Version
Final published version

Citation (APA)
Demiröz, E., Hooijer, G. J., Mulder, F. M., & Urakawa, A. (2026). Beyond competition: hydrogen evolution as a productive pathway in direct toluene hydrogenation. *EES Catalysis*. https://doi.org/10.1039/d6ey00268d

Important note
To cite this publication, please use the final published version (if applicable).
Please check the document version above.

Copyright
In case the licence states “Dutch Copyright Act (Article 25fa)”, this publication was made available Green Open Access via the TU Delft Institutional Repository pursuant to Dutch Copyright Act (Article 25fa, the Taverne amendment). This provision does not affect copyright ownership.
Unless copyright is transferred by contract or statute, it remains with the copyright holder.

Sharing and reuse
Other than for strictly personal use, it is not permitted to download, forward or distribute the text or part of it, without the consent of the author(s) and/or copyright holder(s), unless the work is under an open content license such as Creative Commons.

Takedown policy
Please contact us and provide details if you believe this document breaches copyrights.
We will remove access to the work immediately and investigate your claim.

This work is downloaded from Delft University of Technology.

EES Catalysis

PAPER

Published on 08 October 2026
Licensed under CC-BY 4.0

Check for updates

Cite this: DOI: 10.1039/d6ey00268d

Beyond competition: hydrogen evolution as a productive pathway in direct toluene hydrogenation

Ezgi Demiröz,[ab] Gerben-Jan Hooijer,[a] Fokko M. Mulder[ab] and Atsushi Urakawa*[ab]

Received 4th October 2026,
Accepted 7th October 2026

DOI: 10.1039/d6ey00268d

rsc.li/eescatalysis

The hydrogen evolution reaction (HER) is typically considered a parasitic reaction in electrochemical hydrogenation (ECH) because it reduces the faradaic efficiency toward the desired product. In this work, we investigate the role of HER and conventional thermochemical catalysis in direct toluene hydrogenation coupled with oxygen evolution reaction (OER). We evaluated the electrolysis performance at a fixed current density of 200 mA cm^{-2}, and compared it with systems in which molecular hydrogen was used instead of proton electroreductions. A carefully designed control test showed that the proton conducting cathode catalyst layer, consisting of Pt/C and Nafion ionomer, facilitates both (i) electrochemical HER and (ii) subsequent thermochemical hydrogenation of toluene by utilizing the molecular H_2 produced *in situ*. These findings challenge the common interpretation of ECH of toluene by demonstrating that the process proceeds through an electro-thermochemical mechanism, and thus provide essential insights for the design of energy-efficient hydrogenation processes.

Broader context

Electrification is increasingly viewed as a route to decouple chemical manufacturing from fossil-derived heat and reagents. For electrolyzers to deliver energy savings, however, performance metrics must be carefully linked to the reaction pathway. In this work, we investigate an electrified hydrogenation reaction that connects hydrogen storage with renewable electricity, and reveal the importance of *in situ* generated H_2 utilization over the cathode catalyst layer.

Decarbonizing the chemical industry is essential for meeting climate targets, and powering processes with low-carbon electricity has emerged as an important route to reduce emissions and build a sustainable future.[1–3] Electrification of hydrogenation reactions that are traditionally carried out in thermocatalytic reactors has received considerable attention.[4–9] Electrochemical hydrogenation (ECH) is reported to offer several advantages over the conventional route. First, it generates reactive hydrogen *in situ* from water, thereby eliminating the need to produce, store, and transport molecular hydrogen (H_2).[10–14] Second, it allows performing hydrogenation under milder temperatures and pressures compared to the conventional route.[4,7,10,15–19] Third, targeting compounds with reduction potentials more positive than the competing hydrogen evolution reaction (HER) offers the possibility of achieving higher overall energy efficiencies.[20–22] Despite these benefits, realizing ECH at large scales requires electrolyzers that can operate efficiently at high current densities—a critical challenge for accelerating the transition towards electrochemical processes, which also leads to overpotentials high enough to enable HER.[1,5]

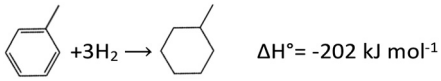
To tackle these challenges, electrolyzers used in industrial-scale applications increasingly employ zero-gap electrolysis systems, in which the electrodes are in direct contact with the membrane. Such systems minimize ohmic losses, enhance mass transport, and allow operation at high substrate concentrations.[7] A successful example is ENEOS Corporation's "Direct MCH" process, demonstrated with 150 kW electrolyzer in Queensland, Australia.[5,23] This project of ENEOS stands as an important milestone, showcasing ECH of neat toluene into methylcyclohexane (MCH), a well-established liquid organic hydrogen carrier.[5]

Conventional toluene hydrogenation involves a two-step process: H_2 production (possibly by water electrolysis) and subsequent hydrogenation in a separate thermocatalytic hydrogenation (TCH) reactor.

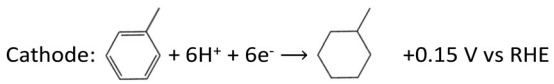
[a] *Department of Chemical Engineering, Faculty of Applied Sciences, Delft University of Technology, Delft, 2629 HZ, The Netherlands. E-mail: a.urakawa@tudelft.nl*
[b] *e-Refinery Institute, Delft University of Technology, Delft, 2628 CB, The Netherlands*

© 2026 The Author(s). Published by the Royal Society of Chemistry

$$3H_2O \rightarrow 3H_2 + 3/2\ O_2 \quad E_{cell}^{\circ} = -1.23\ V,\ \Delta H^{\circ} = +286\ kJ\ mol^{-1}$$



The concept of coupling toluene hydrogenation with OER using membrane electrode assemblies (MEAs) was first introduced by Mitsushima *et al.* in 2015.[20] This approach directly utilizes the protons generated from water, proceeding *via* the following envisaged reactions:



$$\text{Anode: } H_2O \rightarrow 1/2O_2 + 2H^+ + 2e^- \quad + 1.23\ V\ \textit{vs.}\ RHE$$

Researchers employed IrO_2-based catalysts for the OER, Nafion as a proton exchange membrane (PEM), and Pt/C and PtRu/C catalysts at the cathode.[20] Subsequent studies largely adopted the design, exploring Pt group metal catalysts at the cathode in particular[24–30] (Table S1). Notably, Pt-based materials are also highly active for conventional TCH of organic molecules.[31] In addition, Pt-based cathode materials used for ECH are also active for HER due to the shared Volmer-reaction step.[5]

HER uses protons and electrons to generate H_2:

$$\text{Cathode: } 2H^+ + 2e^- \rightarrow H_2 \quad 0\ V\ \textit{vs.}\ RHE$$

Suppression of HER is considered critical for ECH reactions, including CO_2 reduction,[32,33] N_2 reduction,[34,35] NO_x^- reduction,[36] NO reduction,[37,38] organic molecule hydrogenation,[39,40] and transmembrane hydrogenation.[10,41]

In the case of toluene hydrogenation coupled with OER, the ΔG-based theoretical least negative cell potential is −1.08 V,[42] less negative than for water decomposition −1.23 V, while the corresponding ΔH-based thermoneutral potentials are −1.13 and −1.48 V, respectively. Despite this thermodynamic advantage, substantial overpotentials are required in practice. Under the reported conditions for electrochemical toluene hydrogenation, the HER is expected to occur concurrently, as indicated by previous reports[42,43] and the literature summarized in Table S1.

Separately, most anodic oxidation reactions are coupled with HER, where it is considered an auxiliary reaction.[44] Moeller *et al.* utilized this "waste" H_2 in a separate flask for hydrogenation of α,β-unsaturated carboxylic acid with a Pd/C catalyst, showing utilization of on-site generated H_2 for a TCH reaction.[45] Here, the requirement of a separate reactor underscores a key limitation: molecular H_2 must still be handled and reacted *ex situ*. This raises a fundamental question for process design: can the H_2 generated *via* HER be directly utilized *in situ* within an electrochemical reactor? Could this already be happening in electrochemical reactors?

In the electrochemical hydrogenation pathway, active adsorbed hydrogen is generated by proton reduction ($H^+ + e^- \rightarrow H_{ads}$), rather than molecular hydrogen dissociation ($H_2 \rightarrow 2H_{ads}$).[53] Previous works on electrochemical hydrogenation of toluene have extensively focused on electrocatalyst development, and on controlling the competition between ECH and HER.[24,28,29,46–52] However, the effect of *in situ* generated molecular H_2 utilization (TCH) on the proton conducting cathode catalyst layer remained largely unexplored. In this work, we critically evaluate and challenge the conventional view of HER as a competing reaction. To do so, we first examine the electrolysis performance under constant-current operation, where the rate of proton and electron supply is fixed. This allows us to evaluate how the charge is allocated between the products, MCH and H_2.

In a simplified description, direct toluene hydrogenation in a PEM-type electrolyzer proceeds as follows: water oxidizes at the anode to produce oxygen, protons, and electrons. The electrons transfer through an external circuit, whereas the protons migrate across the PEM toward the cathode. At the cathode catalyst, these protons combine with electrons to form adsorbed hydrogen species (H_{ads}). Protons that are not involved in the hydrogenation of toluene into MCH combine and exit the reactor as H_2 gas (Fig. 1a). This process shows high selectivity, with the formation of partially hydrogenated intermediates being negligible.

In electrolysis experiments, catalyst-coated Nafion 115 membranes with a 2 cm × 2 cm active area are used. Catalyst layers consisted of ionomer, Pt/C (2 mg cm^{-2}, 40 wt% Pt) at the cathode and IrO_2 (1 mg cm^{-2}) at the anode. Carbon paper and titanium fiber felt served as the cathode and anode porous transport layers (PTL), respectively (Fig. 1b). Pre-heated toluene and water were continuously supplied to the electrolyzer operating at 80 °C. All measurements were conducted at a current density of 200 mA cm^{-2}. Liquid samples were analyzed using gas chromatography, and the outlet H_2 flow was measured using a gas flow meter (Fig. 1c). A representative chromatogram and the calibration curve are provided in Fig. S1.

To evaluate single-pass conversion, theoretical (maximally achievable) conversion was calculated based on assuming the maximum use of electrons, for the formation of the target product, corresponding to a faradaic efficiency (FE) of 100% toward MCH:

$$X_{th}(\%) = \frac{I \times t \times M_w}{z \times F \times \rho \times Q} \times 100$$

where I is the applied current (A), t is time (s), M_w is the molecular weight of toluene (g mol^{-1}), z is the number of electrons required to hydrogenate one toluene molecule (z = 6), F is Faraday's constant (96 485 C mol^{-1}), ρ is the density of toluene (0.867 g mL^{-1}), and Q is the feed flow rate (mL s^{-1}). This calculation is important to ensure that sufficient protons and electrons are supplied to hydrogenate the target molecule compared to the aimed single-pass conversions.

Fig. 1d compares this theoretical conversion curve with measured conversions across nearly three orders of magnitude in toluene flow rate. Low toluene flow rates yielded high single-pass conversions, reaching 41% at 2 μL min^{-1} with an apparent FE_{MCH} of 10% (Fig. 1e). As expected for continuous-flow operation, the MCH production rate follows the same trend as

© 2026 The Author(s). Published by the Royal Society of Chemistry

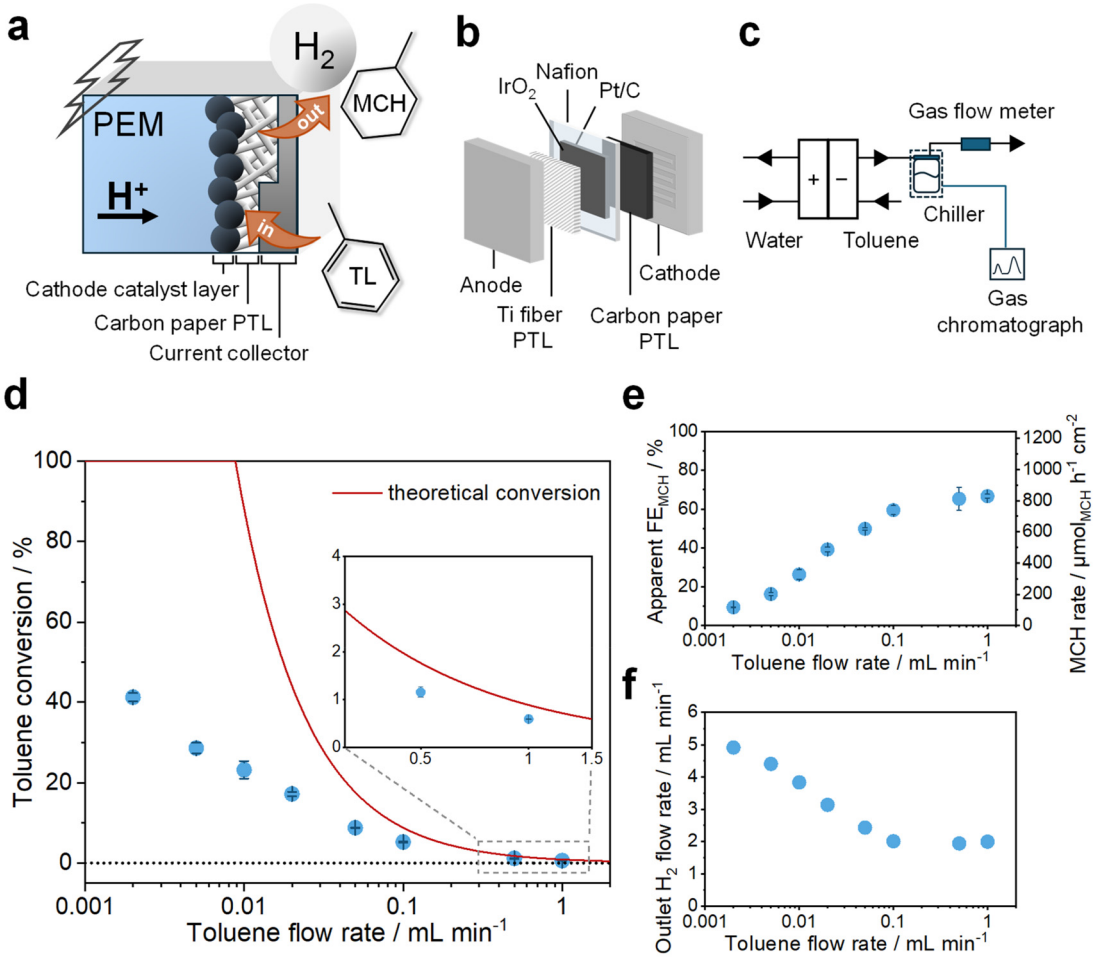


Fig. 1 Electrolysis tests. Schematic of the cathode under electrolysis (a), MEA and current collectors with serpentine flow field (b), schematic of the experimental setup (c), single-pass toluene conversion (d), apparent faradaic efficiency and MCH production rate (e), and outlet H_2 flow rate (f) at 200 mA cm^{-2}, 80 °C, 1.85 mL min^{-1} MilliQ feed at anode.

apparent FE_{MCH}. Increasing toluene flow rate enhances the consumption of adsorbed hydrogen (H_{ads}) for hydrogenation, resulting in higher rates and apparent FE_{MCH}. At toluene flow rates above 0.1 mL min^{-1}, the MCH formation rate approaches a flow-independent value, indicating that the rate is no longer governed by the toluene flow rate. The fraction of protons that have not participated in the hydrogenation reaction appears as measurable H_2 flow at the reactor outlet (Fig. 1f). Throughout the test, cell voltage remained between −1.6 to −1.7 V (Fig. S2, MEA 1). To confirm the reproducibility of the findings, the electrolysis tests were performed with other membrane electrode assemblies (MEAs), as shown in Fig. S2–S4. Total FE in the tests, as well as water drag rate from the anode due to electroosmosis, are given in Fig. S5.

Electrolysis results show that a substantial fraction of the cathodic current leads to molecular H_2. Since Pt-based catalysts are active for TCH of organic compounds, the locally generated H_2 may, in principle, be utilized within the same catalyst layer before leaving the reactor. Therefore, a control experiment is carefully designed to evaluate the thermocatalytic activity of the catalyst layer (Fig. 2a and b). The H_2 gas flow rate was set at 5.6 mL min^{-1}, the same as the H_2 flow rate measured at the outlet when toluene is not introduced to the cathode (water electrolysis operation at 800 mA, 4 cm^2, 92% FE). This way, the inlet H_2 flow rate can be considered equivalent to the amount of H_2 generated *in situ* by electrochemical HER. The anode is continuously flushed with inert N_2 to ensure open circuit potential of 0 V during tests to avoid any potential polarization and charging effect on the catalyst. For a better comparison, an electrolysis test was performed before switching to the control test using the same MEA (Fig. 2c). Notably, similar toluene conversions of about 20% are observed in both cases, indicating that a Nafion-containing Pt/C catalyst layer thermochemically utilizes *in situ* generated H_2. More control experiments on different MEAs are given in Fig. S6 and S7.

Arrhenius relationship can reveal the factors controlling reaction rates in chemically driven *versus* electrically driven processes, as the reaction mechanisms and thus kinetic parameters are expected to be distinct. Such comparisons have been reported by Lercher and co-workers, who examined hydrogenation rates by increasing hydrogen chemical potential either through elevated H_2 pressure or by applying a cathodic

© 2026 The Author(s). Published by the Royal Society of Chemistry

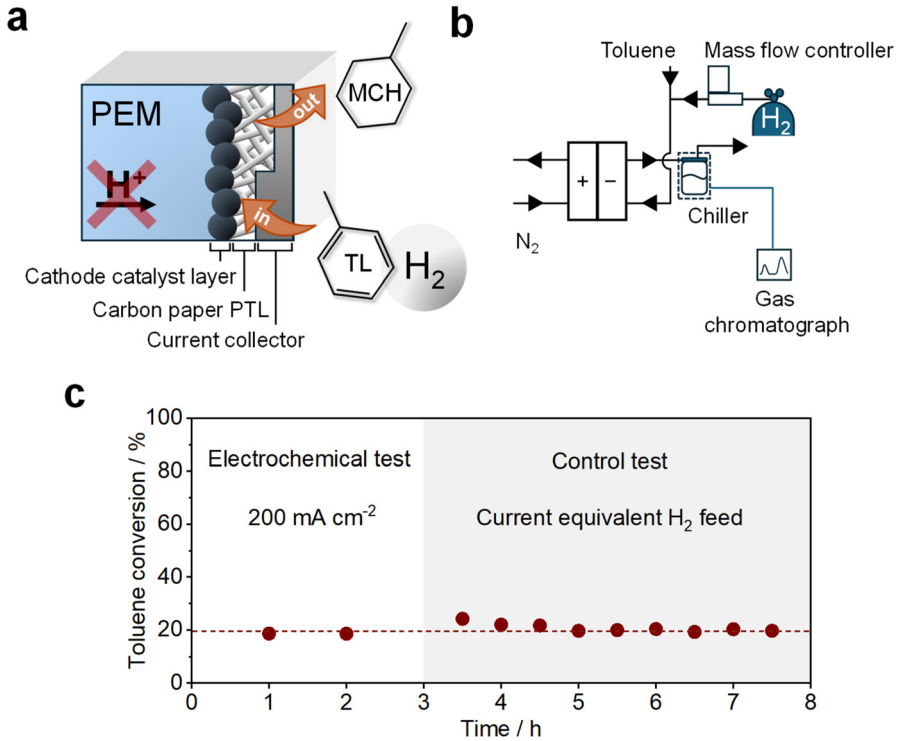


Fig. 2 Control test. Schematic of cathode during the control test (a), schematic of experimental setup (b) and single-pass toluene conversion comparisons (c) at 200 mA cm^{-2}/5.6 mL min^{-1} H_2 feed, 80 °C, 5 μL min^{-1} toluene.

potential.[54–56] In contrast, our approach does not treat HER as a competing pathway. Instead of controlling the cathodic potential, we control current density to fix the H_2 generation at the cathode. During experiments, temperature is varied between 50 and 80 °C, within Nafion's operation range. For the TCH, a packed bed reactor is designed for the analysis (Fig. S8 and S9). To eliminate temperature control-related differences between experiments, the catalyst bed is placed inside the electrolyzer. For a fair comparison between the electrolysis test, a catalyst bed is prepared using dried catalyst ink having the same composition as that used for MEA preparation. Nafion ionomer served as a binder to pelletize Pt/C catalyst, which was further sieved in the range of 56–100 μm. Similar to the control test, 5.6 mL min^{-1} H_2 was fed with toluene. The toluene flow rate was selected from regimes in which the MCH formation rate was nearly independent of toluene feed rate, corresponding to 2 mL min^{-1} for electrolysis, and 0.5 mL min^{-1} for the thermocatalytic test (Fig. S10).

If ECH were the dominant and kinetically distinct pathway, a different temperature dependence might be expected compared with TCH. Instead, Fig. 3 shows that the two systems exhibit practically no difference in apparent activation energy. However, measured values of approximately 20 kJ mol^{-1} are substantially lower than those typically reported for toluene hydrogenation over Pt nanoparticle catalysts under comparable temperature conditions, which are around 50 kJ mol^{-1} within a comparable temperature range.[57] This unusually low apparent activation energies may indicate that both systems are influenced by similar internal mass-transfer limitations, where reactants cannot move fast enough inside the pores of the catalyst particle, biasing the activation energy to close to the half. Such limitations may originate from the Nafion binder phase occupying the catalyst pores, which can weaken the temperature dependence of the measured reaction rate.

For hydrogenation proceeding through an electro-thermochemical pathway, increasing the cathode pressure is expected to promote product formation according to Le Chatelier's principle, without producing a clear voltage response. In this test, we pressurize the cathode to 6 barg using a back pressure regulator attached to the outlet of the electrolyzer. As shown in Fig. 4, during the first 35 min, the cell was operated without cathode

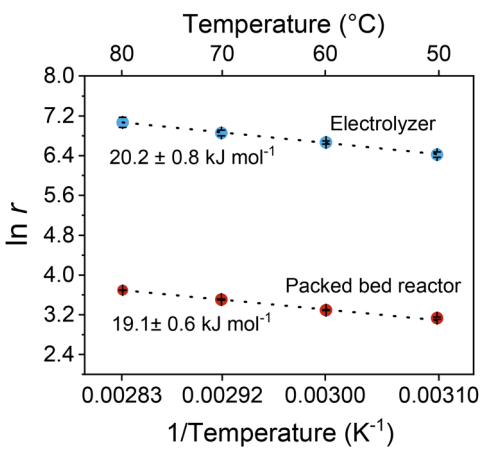


Fig. 3 Arrhenius analysis comparison. Electrolysis performed at 200 mA cm^{-2}, thermal catalysis performed with 5.6 mL min^{-1} H_2.

© 2026 The Author(s). Published by the Royal Society of Chemistry

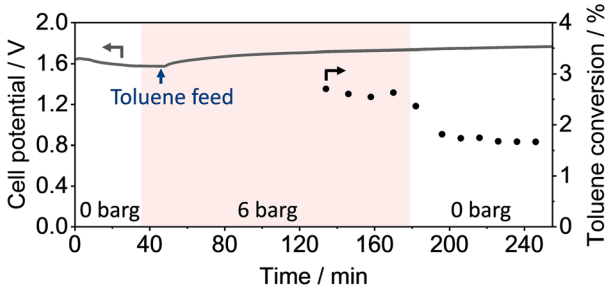


Fig. 4 Effect of cathode pressure on toluene hydrogenation. Electrolysis performed at 200 mA cm^{-2}, 80 °C.

pressurization or toluene flow, during which the cell potential decreased and stabilized due to membrane hydration. The cathode was then pressurized, and toluene was introduced at 0.1 mL min^{-1} at *ca.* 43 min, and sampling started after 2 h. Under pressure, the toluene conversion was *ca.* 2.8%. Upon pressure release at 3 h, the conversion decreased to *ca.* 1.8%.

Both the control experiment and Arrhenius analysis confirm that the Pt/C-Nafion cathode catalyst layer is active for thermochemical hydrogenation and can achieve identical single-pass toluene conversion and apparent activation energies as the electrolysis operation. This result is consistent with the well-established role of Pt as not only an effective HER and ECH catalyst, but also a benchmark catalyst for aromatic hydrogenation using molecular hydrogen.[58]

Most catalysis and modelling studies treat proton-conducting catalyst layers as electrodes that are active for electrochemical hydrogenation and HER.[30,59] Considering there are no reports showing 100% FE_{MCH} at conditions where HER is not thermodynamically expected, we believe such hydrogenation reactions may not all be classified purely as electrochemical. Accordingly, faradaic efficiency in such systems should be regarded as *apparent faradaic efficiency*, reflecting electrical utilization rather than the underlying chemical mechanism.

In the control test, zero-gap type cell architecture enabled direct exposure of the catalyst layer to molecular hydrogen. For H-cells or flow cells with gaps between components, ensuring H_2 availability near the electrode could be troublesome. This is consistent with our previous PEM-based nitrate reduction study where externally supplied H_2 was much less effective than electrolysis-assisted operation.[60]

Architectural dependence highlights a broader challenge in electrocatalysis, where reactions are often evaluated across different cell configurations, such as transitioning from H-cells to zero-gap systems or *vice versa*. We speculate that, if a reaction is partially or predominantly promoted by *in situ* generated H_2, differences in H_2 transport and accessibility between these configurations may lead to divergent activity and selectivity trends. As a result, performance metrics obtained in different reactor designs may not be directly comparable. Furthermore, cell construction factors (cell and gasket architecture, compression, *etc.*) in zero-gap assemblies become highly important.

From an energetic perspective, the necessity of HER implies that operation at less negative cell potentials than the thermodynamic water-splitting potential is unlikely. Nonetheless, the process may still offer great system-level advantages, as the exothermic hydrogenation reaction can provide internal heat, and H_2 generation and consumption occur in a single integrated device without external handling of H_2. Even though both reactors are not optimized, we observed that MCH production rate (per gram of catalyst) of direct hydrogenation can be higher than that of the H_2-fed packed bed reactor (Fig. S10). In addition, using electrolyte-free water at the anode as the hydrogen source simplifies system design and improves relevance for practical implementation. A future system-level comparison with conventional water electrolysis followed by thermocatalytic hydrogenation would help clarify the practical advantages of the integrated system.

Conclusions

Our work demonstrates that HER contributes productively to direct toluene hydrogenation in PEM type electrolyzers. In the Pt/C–Nafion cathode catalyst layer, electrochemically generated molecular H_2 is consumed *in situ* for thermochemical hydrogenation to methylcyclohexane, rather than simply leaving the reactor as an efficiency loss. The comparable performance observed in the electrolysis and H_2-fed control experiments indicates that thermochemical hydrogenation takes place under the investigated conditions. In such systems, observed faradaic efficiencies should be interpreted as measures of how effectively electrical input is converted into the target product, rather than as direct evidence of the elementary hydrogenation pathway. Recognizing this distinction provides a more reliable basis for interpreting and designing integrated electrified hydrogenation processes.

Author contributions

E. D.: conceptualization, investigation, methodology, formal analysis, visualization, writing – original draft. G. J. H.: investigation, formal analysis. F. M. M.: supervision, writing – review & editing. A. U.: supervision, writing – review & editing.

Conflicts of interest

There are no conflicts to declare.

Data availability

The data supporting this article are available in the supplementary information (SI) and in the 4TU.ResearchData repository at https://doi.org/10.4121/557eac7f-cd6c-4ee8-8fcc-29c798777f98. See DOI: https://doi.org/10.1039/d6ey00268d.

© 2026 The Author(s). Published by the Royal Society of Chemistry

Acknowledgements

All authors acknowledge the financial support from Horizon-EIC, Pathfinder Challenges (Grant 101070976). The authors also thank Eunhye (Grace) Choi for performing SEM imaging.

References

1 D. S. Mallapragada, Y. Dvorkin, M. A. Modestino, D. V. Esposito, W. A. Smith, B.-M. Hodge, M. P. Harold, V. M. Donnelly, A. Nuz, C. Bloomquist, K. Baker, L. C. Grabow, Y. Yan, N. N. Rajput, R. L. Hartman, E. J. Biddinger, E. S. Aydil and A. D. Taylor, *Joule*, 2023, **7**, 23–41.
2 P. Mayer, F. J. Baader, D. Y. Shu, L. Leenders, C. Zibunas, S. Moret and A. Bardow, *Energy Environ. Sci.*, 2025, **18**, 7967–7979.
3 G. Papanikolaou, G. Centi, S. Perathoner and P. Lanzafame, *ACS Catal.*, 2022, **12**, 2861–2876.
4 B. K. Kundu and Y. Sun, *Chem. Sci.*, 2024, **15**, 16424–16435.
5 J. T. Kleinhaus, J. Wolf, K. Pellumbi, L. Wickert, S. C. Viswanathan, K. Junge Puring, D. Siegmund and U.-P. Apfel, *Chem. Soc. Rev.*, 2023, **52**, 7305–7332.
6 Y. Wang, Q. Wang, L. Wu, K. Jia, M. Wang and Y. Qiu, *Nat. Commun.*, 2024, **15**, 2780.
7 K. Pellumbi, L. Wickert, J. T. Kleinhaus, J. Wolf, A. Leonard, D. Tetzlaff, R. Goy, J. A. Medlock, K. Junge Puring, R. Cao, D. Siegmund and U.-P. Apfel, *Chem. Sci.*, 2022, **13**, 12461–12468.
8 J. Jankovic and D. P. Wilkinson, *Can. J. Chem. Eng.*, 2024, cjce.25549.
9 G. Han, G. Li and Y. Sun, *Nat. Catal.*, 2023, **6**, 224–233.
10 X. Zhou, X. Yu, B. You and Y. Jing, *J. Mater. Chem. A*, 2024, **12**, 20527–20541.
11 B. Li and H. Ge, *Sci. Adv.*, 2019, **5**, eaaw2774.
12 C. Liu, Y. Wu, B. Zhao and B. Zhang, *Acc. Chem. Res.*, 2023, **56**, 1872–1883.
13 G. Han, G. Li and Y. Sun, *Nat. Catal.*, 2023, **6**, 224–233.
14 Y. Wen, M. D. Stankovic, A. Singha Hazari, M. L. Frisch, S. Ma and C. P. Berlinguette, *Energy Environ. Sci.*, 2025, **18**(14), 7223–7230.
15 R. S. Sherbo, R. S. Delima, V. A. Chiykowski, B. P. MacLeod and C. P. Berlinguette, *Nat. Catal.*, 2018, **1**, 501–507.
16 Z. Shi, N. Li, H.-K. Lu, X. Chen, H. Zheng, Y. Yuan and K.-Y. Ye, *Curr. Opin. Electrochem.*, 2021, **28**, 100713.
17 M. D. Chilunda, S. A. Talipov, H. M. U. Farooq and E. J. Biddinger, *ACS Sustainable Chem. Eng.*, 2025, **13**, 1174–1195.
18 M. Zhou, Y. Miao, Y. Gu and Y. Xie, *Adv. Mater.*, 2024, **36**, 2311355.
19 M. D. Stankovic, N. E. LeSage, J. F. Sperryn, A. Kurimoto and C. P. Berlinguette, *ACS Energy Lett.*, 2024, **9**, 4459–4464.
20 S. Mitsushima, Y. Takakuwa, K. Nagasawa, Y. Sawaguchi, Y. Kohno, K. Matsuzawa, Z. Awaludin, A. Kato and Y. Nishiki, *Electrocatalysis*, 2016, **7**, 127–131.
21 Y. Inami, H. Ogihara and I. Yamanaka, *ChemistrySelect*, 2017, **2**, 1939–1943.
22 N. Itoh, W. C. Xu, S. Hara and K. Sakaki, *Catal. Today*, 2000, **56**, 307–314.
23 Direct MCH®|Carbon Neutrality|RESEARCH & DEVELOPMENT|R&D Special Website, https://www.eneos.co.jp/english/rd/research/carbon-neutral/dmch.html, (accessed October 9, 2026).
24 L. Zheng, L. Zhang, J. Bai, Y. Zhang, S. Wei, C. Zhang, G. Zhang, Y. Ma, X. Wang and Y. Jia, *Small*, 2025, 2501665.
25 F. I. Reyna-Peña, A. Atienza-Márquez, S. Jang, K. Shigemasa, R. Shiono, K. Nagasawa, T. Araki and S. Mitsushima, *Renewable Energy*, 2025, **240**, 122223.
26 J. Park, J. Jeon, Y. Yoon and T. Lim, *J. Electrochem. Sci. Technol.*, 2025, **16**, 160–170.
27 C. J. Lee, T. Kim, J. Song, S. J. Yoon, K.-H. Oh, D. M. Yu, S.-Y. Lee and S. So, *J. Mater. Chem. A*, 2025, **13**(6), 4090–4099.
28 C.-H. Chan, C.-K. Hwang, N. Tamir, H. Nam, S. Y. Paek, J. Lim, B. Ulambayar, K. H. Chae, W. Sun, S. A. Akhade, G. Bucci, S. Y. Lee, J. M. Kim, S.-H. Cho and S. S. Han, *ACS Catal.*, 2025, **15**, 13667–13677.
29 Y. Inami, H. Ogihara, S. Nagamatsu, K. Asakura and I. Yamanaka, *ACS Catal.*, 2019, **9**, 2448–2457.
30 K. Nagasawa, Y. Sawaguchi, A. Kato, Y. Nishiki and S. Mitsushima, *Electrochemistry*, 2018, **86**, 339–344.
31 Z. Jing, Y. Guo, Q. Wang, X. Yan, G. Yue, Z. Li, H. Liu, R. Qin, C. Zhong, M. Li, D. Xu, Y. Yao, Y. Yao and M. Shuai, *Nat. Commun.*, 2024, **15**, 5806.
32 X. Yu, Y. Xu, L. Li, M. Zhang, W. Qin, F. Che and M. Zhong, *Nat. Commun.*, 2024, **15**, 1711.
33 Q. Li, X. You, J. Wu and Z. Tang, *Adv. Funct. Mater.*, 2025, e08825.
34 C. Choi, G. H. Gu, J. Noh, H. S. Park and Y. Jung, *Nat. Commun.*, 2021, **12**, 4353.
35 X. Long, F. Huang, Z. Yao, P. Li, T. Zhong, H. Zhao, S. Tian, D. Shu and C. He, *Small*, 2024, **20**, 2400551.
36 W. Liu, Y. Lv, H. Ou, J. Zhang, Y. Ren, M. Xia, Y. Li, H. Li, X. Ren, H. Hu and G. Yang, *Nat. Commun.*, 2025, **16**, 5716.
37 G. Gan, G. Hong and W. Zhang, *Adv. Funct. Mater.*, 2024, 2401472.
38 S. Bunea, M. Coppens and A. Urakawa, *ACS Catal.*, 2023, **13**, 11345–11351.
39 C. Liu, Y. Wu, B. Zhao and B. Zhang, *Acc. Chem. Res.*, 2023, **56**, 1872–1883.
40 G. Durin, N. Kaeffer and W. Leitner, *Curr. Opin. Electrochem.*, 2023, **41**, 101371.
41 M. D. Stankovic, N. E. LeSage, J. F. Sperryn, A. Kurimoto and C. P. Berlinguette, *ACS Energy Lett.*, 2024, **9**, 4459–4464.
42 K. Nagasawa and S. Mitsushima, *J. Jpn. Petrol. Inst.*, 2024, **67**, 97–104.
43 J. Zhu, T. Hartung, D. Tegtmeyer, H. Baltruschat and J. Heitbaum.
44 T. Wu and K. D. Moeller, *Angew. Chem.*, 2021, **133**, 12993–13000.
45 T. Wu, B. H. Nguyen, M. C. Daugherty and K. D. Moeller, *Angew. Chem., Int. Ed.*, 2019, **58**, 3562–3565.

 © 2026 The Author(s). Published by the Royal Society of Chemistry

46 A. A. H. Tajuddin, T. Ohto, H. Tanimoto, T. Fujita, S. Jeong, A. Fukazawa, Y. Shimoyama, Y. Misu, K. Takano, K. Matsuoka and Y. Ito, *ChemSusChem*, 2025, **18**, e202401071.
47 T. Imada, Y. Iida, Y. Ueda, M. Chiku, E. Higuchi and H. Inoue, *Catalysts*, 2021, **11**, 318.
48 Y. Inami, S. Iguchi, S. Nagamatsu, K. Asakura and I. Yamanaka, *ACS Omega*, 2020, **5**, 1221–1228.
49 T. Imada, M. Chiku, E. Higuchi and H. Inoue, *ACS Catal.*, 2020, **10**, 13718–13728.
50 Y. Inami, H. Ogihara and I. Yamanaka, *Electrocatalysis*, 2018, **9**, 204–211.
51 E. Higuchi, Y. Ueda, M. Chiku and H. Inoue, *Electrocatalysis*, 2018, **9**, 226–235.
52 Y. Inami, H. Ogihara and I. Yamanaka, *ChemistrySelect*, 2017, **2**, 1939–1943.
53 *Encyclopedia of Applied Electrochemistry*, ed. G. Kreysa, K. Ota and R. F. Savinell, Springer New York, New York, NY, 2014.
54 Y. Song, O. Y. Gutiérrez, J. Herranz and J. A. Lercher, *Appl. Catal., B*, 2016, **182**, 236–246.
55 U. Sanyal, Y. Song, N. Singh, J. L. Fulton, J. Herranz, A. Jentys, O. Y. Gutiérrez and J. A. Lercher, *ChemCatChem*, 2019, **11**, 575–582.
56 N. Singh, Y. Song, O. Y. Gutiérrez, D. M. Camaioni, C. T. Campbell and J. A. Lercher, *ACS Catal.*, 2016, **6**, 7466–7470.
57 S. D. Lin and M. A. Vannice, *J. Catal.*, 1993, **143**, 554–562.
58 S. Ramadhani, Q. N. Dao, Y. Imanuel, M. Ridwan, H. Sohn, H. Jeong, K. Kim, C. W. Yoon, K. H. Song and Y. Kim, *ChemCatChem*, 2024, **16**, e202401278.
59 V. M. Ehlinger, T. Chatterjee, S. Deo, M. Yuan, G. Bucci, M. J. McNenly and S. A. Akhade, *J. Electrochem. Soc.*, 2025, **172**, 114505.
60 J. Ampurdanés, S. Bunea and A. Urakawa, *ChemSusChem*, 2021, **14**, 1534–1544.

© 2026 The Author(s). Published by the Royal Society of Chemistry